Characterization of Lipid Binding Specificities of Dysferlin C2 Domains Reveals Novel Interactions with Phosphoinositides†

Christian Therrien, Sabrina Di Fulvio, Sarah Pickles, and Michael Sinnreich*

Neuromuscular Research Group, Montreal Neurological Institute and Hospital, McGill University, Montreal, Canada

Received December 8, 2008; Revised Manuscript Received January 13, 2009

ABSTRACT: Dysferlin is a type II transmembrane protein implicated in Ca^{2+}-dependent sarcolemmal membrane repair. Dysferlin has seven C2 domains, which are lipid and protein binding modules. In this study, we sought to characterize the lipid binding specificity of dysferlin's seven C2 domains. Dysferlin's C2A domain was able to bind to phosphatidylserine (PS), phosphatidylinositol 4-phosphate [PtdIns(4)P], and phosphatidylinositol 4,5-bisphosphate [PtdIns(4,5)P_2] in a Ca^{2+}-dependent fashion. The remainder of the C2 domains exhibited weaker and Ca^{2+}-independent binding to PS and no significant binding to phosphoinositides.

Mutations in the dysferlin gene lead to limb-girdle muscular dystrophy 2B (*1*), Miyoshi myopathy (*2*), and distal anterior compartment myopathy (*3*). Muscle fibers from dysferlin deficient mice are unable to efficiently repair membrane tears caused by normal muscle contraction or by induced injuries (*4*). Dysferlin is a large type II transmembrane protein composed of seven C2 domains and two Dysf domains (*5*). Dysferlin is found predominantly in the sarcolemma and the T-tubular system of muscle fibers (*6*). Its interactions with lipids and proteins are likely mediated by the C2 domains. C2 domains are found in a plethora of proteins implicated in vesicular trafficking, membrane binding, or cellular signaling (*7*−*11*). Multiple-C2 domain proteins, like the synaptotagmins and the ferlins, are involved in membrane interactions. The C2 domain structure shares a conserved fold of eight-stranded antiparallel β-sheets forming a sandwich structure that is connected by surface loops (*12*). The lipid binding activity of C2 domains can be Ca^{2+}-dependent or -independent. The Ca^{2+}-regulated activity is defined structurally by the presence of conserved aspartic acid residues located in the loops interposed between the β-sheets. The role of these residues is to properly coordinate the Ca^{2+} ions to establish a positive electrostatic environment or to interact directly with the phosphate group of anionic lipids. The C2A domain of the dysferlin homologue, myoferlin, was shown to bind to phosphatidylserine/phosphatidylcholine liposomes in a Ca^{2+}-dependent manner, whereas the other myoferlin C2 domains failed to exhibit any binding activity (*13*). The C2D domain of another dysferlin homologue, otoferlin, was shown to bind Ca^{2+} by fluorescence emission spectroscopy (*14*), but no lipid binding studies were reported. The dysferlin C2A domain was also tested with a liposome centrifugation assay and exhibited PS/PC[1] binding activity only in the presence of Ca^{2+} (*13*). The lipid binding activity and specificity of the other dysferlin C2 domains have not been characterized to date. Here, we present the characterization of the lipid specificity and Ca^{2+} dependency of all seven dysferlin C2 domains. We also expand the characterization of the dysferlin C2A domain using screening arrays composed of biologically relevant lipids.

EXPERIMENTAL PROCEDURES

Cloning of Dysferlin C2 Domains. To clone the coding sequence of complete and functional dysferlin C2 domains, we took into account the in silico predictions regarding type I or type II topologies of the C2 domains since no crystal coordinates of dysferlin C2 domains are available. We previously predicted that the C2A, C2B, and C2E domains could adopt the type II topology, whereas the remainder of the C2 domains were expected to adopt the type I topology (*5*). We used a sequence alignment of dysferlin C2 domains along with secondary structure information obtained from synaptotagmin III C2A and protein kinase C δ C2 crystal structures to map the putative calcium binding residues and structurally conserved residues (Figure 1). The selection of residues important for the structure of the β-strands was further refined using a consensus of residues obtained from the sequence alignment of 65 published C2 domains of both topologies (*15*). On the basis of this sequence information, we included residues predicted to generate the first and last

† Financial support from the CIHR-ALS-MDAC (Grant 85076) partnership program, AFM (Grant 12956), and FRSQ (Award 13986) is gratefully acknowledged.

* To whom correspondence should be addressed: Montreal Neurological Institute and Hospital, 3801 University St., Montreal, Quebec H3A 2B4, Canada. E-mail: michael.sinnreich@mcgill.ca. Phone: (514) 398-8528. Fax: (514) 398-8310.

[1] Abbreviations: PS, phosphatidylserine; PC, phosphatidylcholine; PtdIns(3)P, phosphatidylinositol 3-phosphate; PtdIns(4)P, phosphatidylinositol 4-phosphate; PtdIns(5)P, phosphatidylinositol 5-phosphate; PtdIns(4,5)P_2, phosphatidylinositol 4,5-bisphosphate; PI4P5K, phosphatidylinositol 4-phosphate 5-kinase; IPTG, isopropyl β-D-1-thiogalactopyranoside; GST, glutathione *S*-transferase; BSA, bovine serum albumin; TBST, Tris-buffered saline with Tween 20; PLO, protein−lipid overlay assay; LUV, large unilamellar vesicles; TGN, trans Golgi network; SV, secretory vesicles; EGTA, ethylene glycol bis(2-aminoethyl)-*N*,*N*,*N*′,*N*′-tetraacetic acid; PKC, protein kinase C; MDCK, Madin-Darby canine kidney; FAPP, four-phosphatase-adaptor protein; CERT, ceramide transfer protein.

10.1021/bi802242r CCC: $40.75
Published on Web 03/02/2009

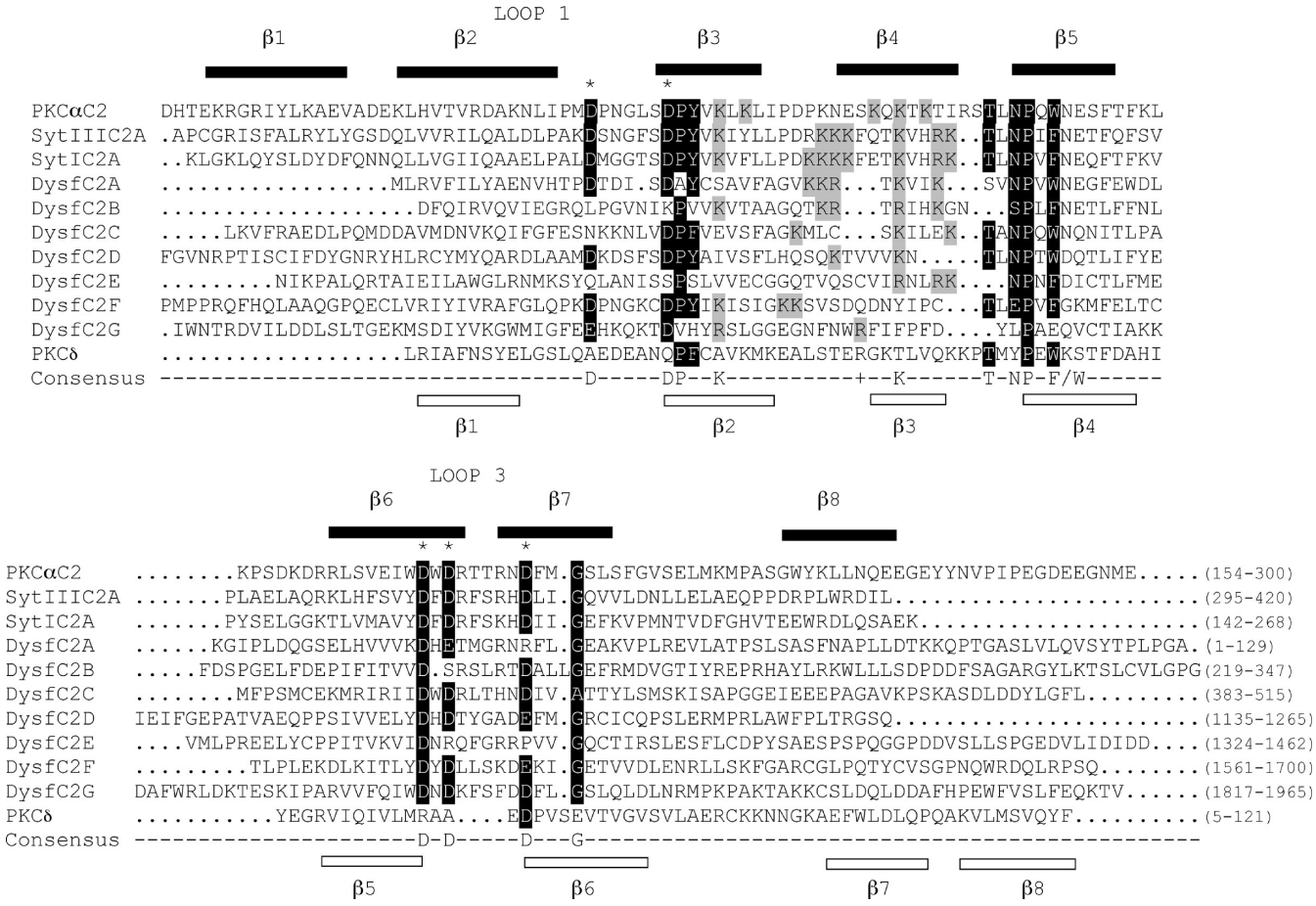

FIGURE 1: Multiple-sequence alignments of the seven C2 domains of human dysferlin along with the type I topology C2A domain of the mouse synaptotagmin III [Protein Data Bank (PDB) entry 1DQV], the type II topology C2 domain of rat protein kinase C δ (PDB entry 1BDY), the C2 domain of human protein kinase C α (GenBank entry NP_002728), and the C2A domain of human synaptotagmin I (GenBank entry NP_005630). Asterisks indicate the location of aspartic acid residues implicated in Ca^{2+} coordination. The secondary structures found in the crystal structure of the C2 domains of synaptotagmin III and protein kinase C δ (type I and II topologies) are depicted either above or below the sequences. Residue numbers used for the alignment are in parentheses at the end of the sequences. Conserved residues are highlighted in black, and positively charged residues in the polybasic region are highlighted in gray.

β-strands of the putative C2 domain structure (C2A, C2B, and C2D), and in some instances, we extended the boundaries to provide more stability to the construct or alternatively to include all secondary elements (first and last β-strands of types I and II, respectively) in the case of possible biased topology predictions (C2C, C2E, C2F, and C2G). The seven C2 domains of dysferlin were amplified by PCR using the human dysferlin cDNA cloned in the DFL-2 plasmid (kindly provided by K. Bushby, Newcastle, U.K.) and Klentaq polymerase (Sigma). The C2A domain for human synaptotagmin I (GenBank entry NM_005639.1) was amplified from a commercially available cDNA clone (Origene). *Eco*RI and *Bam*HI sites were included in the primer sequences to subclone the fragments in frame with glutathione *S*-transferase (GST) in the multiple cloning site of pGEX4T1 (GE Healthcare) to generate eight GST fusion proteins (Figure 2). All recombinant constructs were verified by DNA sequencing.

Expression and Purification of Dysferlin C2 Domains. All the clones were expressed in *Escherichia coli* BL-21. One isolated colony was used to inoculate 10 mL of 2× YT medium (BioShop) containing 100 μg/mL ampicillin and incubated overnight at 37 °C. This overnight culture was subsequently transferred to 500 mL of medium and incubated at 37 °C until the optical density at 600 nm reached 0.5. The expression of fusion protein was induced by the addition of IPTG to a final concentration of 0.5 mM followed by incubation at 26 °C for 2 h with vigorous shaking (225 rpm). The cells were collected at 6000 rpm and kept frozen at −80 °C until needed. The cells were thawed and resuspended in 1 mL of ice-cold lysis buffer [20 mM Tris-HCl (pH 7.5), 150 mM NaCl, 1 mg/mL DNase, 1× protease inhibitor cocktail (Roche), and 1 mg/mL lysozyme], incubated for 10 min on ice, and then further lysed by three rounds of sonication of 15 s each on ice at an intensity of 3.5 (Vibrocell, Sonics). Lysates were incubated for 30 min at 4 °C with 1% Triton X-100 and centrifuged at 20000*g* for 30 min at 4 °C. The soluble fractions were incubated with 300 μL of a 50% glutathione Sepharose 4B suspension (GE Healthcare) for 2 h on a rotating platform. The suspension was centrifuged, and the beads were washed five times with lysis buffer without lysozyme and DNase. The GST fusion proteins were eluted at room temperature with 10 mM reduced glutathione (GE Healthcare) in 50 mM Tris-HCl (pH 8.0). The eluates were divided into aliquots and stored at 4 °C. Protein concentrations were determined with a Bradford protein assay. Protein purity and size were analyzed by SDS−PAGE.

Protein−Lipid Overlay Assay (PLO). Lipid binding specificity was assessed with protein−lipid overlay assays using

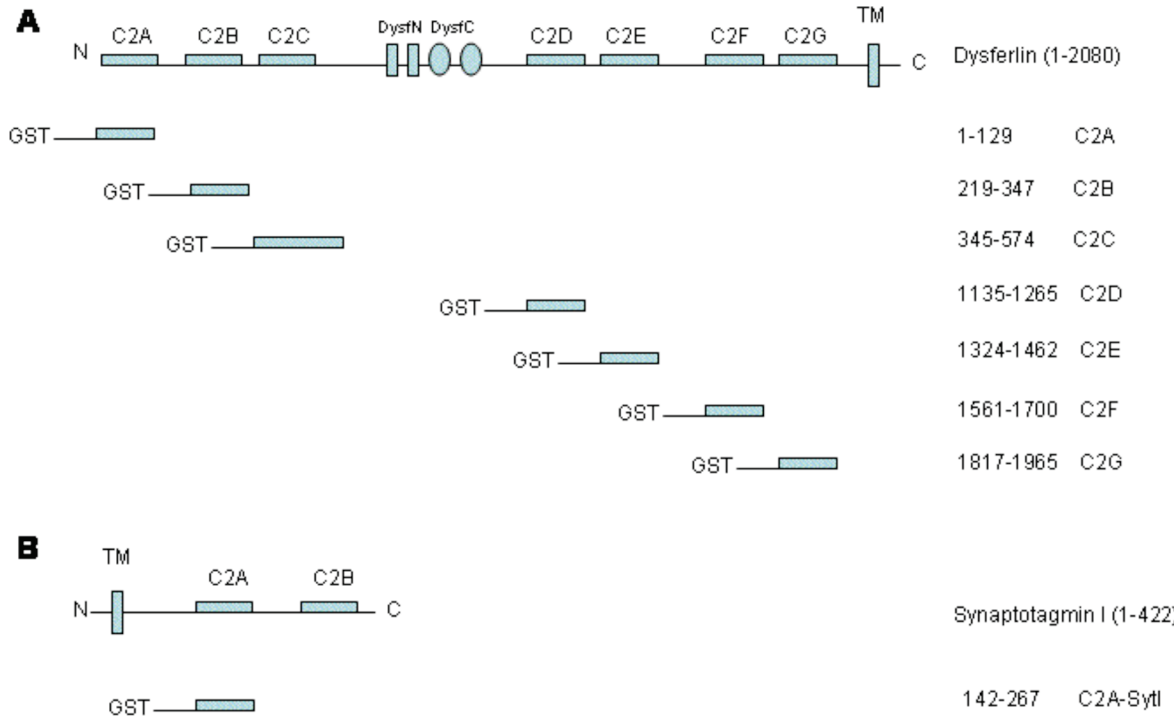

FIGURE 2: Dysferlin and synaptotagmin I GST−C2 domain fusion proteins used in this study. The numbering of residues included in the recombinant proteins is shown in parentheses.

commercially available lipid strips blotted with 100 pmol of biologically relevant lipids (Echelon Biosciences). Custom lipid strips were also prepared in our laboratory using larger amounts of lipids to increase the sensitivity of the binding assay. Several dilutions of chloroform/methanol/water (1:2:0.8) solutions of PS, PtdIns(4)P, or PtdIns(4,5)P_2 (Avanti Polar Lipids Inc.) were spotted onto Trans-Blot nitrocellulose membranes (Bio-Rad) and air-dried.

Lipid strips were blocked with 3% fatty acid-free BSA (Sigma) in TBST for 1 h at room temperature and then incubated with 0.5 μg/mL soluble GST−C2 domain fusion proteins in TBST for 16 h at 4 °C. The following day, the blots were washed three times with TBST for 10 min followed by incubation with a 1:5000 dilution of anti-GST antibodies (GE Healthcare) in TBST for 1 h at room temperature. The membranes were washed as previously described, incubated with a 1:5000 dilution of anti-goat horseradish peroxidase conjugate (Zymed), and subsequently washed extensively with TBST over a period of 1 h. The protein−lipid interactions were detected by enhanced chemiluminescence (Amersham).

Phospholipid Centrifugation Binding Assay. The preparation of large unilamellar vesicles (LUV) was performed according to reported methods (*16*). Chloroform solutions composed of 35% PC and 65% PS, 80% PC and 20% PtdIns(4)P, or 80% PC and 20% PtdIns(4,5)P_2 were mixed and dried under a stream of nitrogen gas. The dried lipid films were resuspended in buffer A [50 mM HEPES-NaOH (pH 6.8), 100 mM NaCl, and 4 mM Na_2EGTA] containing 0.5 M sucrose, subjected to five freeze−thaw cycles, and passed several times through a 0.1 μm filter (Whatman) using the Mini-Extruder instrument (Avanti Polar Lipids Inc.) to produce homogeneously sized 100 μm liposomes (LUV).

For the binding assay, soluble GST-C2 domain fusion proteins (5 μg) were mixed with LUV (100 μg) in buffer A with Ca^{2+}/EGTA buffers whose composition was calculated with WEBMAXCLITE version 1.15 (www.stanford.edu/cpatton/webmax). The mixture was incubated for 30 min at room temperature and centrifuged at 100000*g* for 30 min in a TLA-100 ultracentrifuge (Beckman Instruments). Supernatant (soluble fraction) and pellet fractions were collected and analyzed by SDS−PAGE. Protein bands were stained with SimplyBlue SafeStain (Invitrogen) for 1 h and washed in water. Gels were scanned with an Epson Perfection 4490 Photo Scanner, and densitometric analysis of the protein bands was performed with NIH ImageJ version 1.41. The percentages of lipid bound protein were calculated with the equation % of lipid-bound protein = pellet fraction/(pellet fraction + soluble fraction) × 100. The gel data presented for the Ca^{2+} titration experiments consisted of the lipid-bound protein fractions only and a total protein control (input). We used the terminology of Ca^{2+} apparent affinity to describe the lowest concentration of Ca^{2+} at which strong lipid binding is detectable, which is distinguishable from nonspecific binding in Ca^{2+} titration experiments, as described previously by others (*8, 10, 17*).

RESULTS

Dysferlin C2 Domains Bind to Phosphatidylserine through Ca^{2+}-Dependent and -Independent Mechanisms. All dysferlin GST−C2 domain fusion proteins were successfully expressed in *E. coli* and purified by affinity chromatography with glutathione Sepharose. Lipid binding selectivity was determined for all C2 domains using lipid strips blotted with several biologically relevant lipids found in mammalian cells (Figure 3A). The C2A domains of both synaptotagmin I and dysferlin showed binding to PS and several phosphoinositide monophosphates in a Ca^{2+}-dependent fashion (Figure 3B). All of the other dysferlin C2 domains exhibited no detectable or weak binding (C2F) to PS and phosphoinositide monophosphate (Figure 3B). None of the C2 domains exhibited

A

Lysophosphatidic Acid (LPA)	○	○	Sphingosine-1-phosphate (S1P)
Lysophosphocholine (LPC)	○	○	PtdIns(3,4)P_2 (P-3416)
PtdIns (P-0016)	○	○	PtdIns(3,5)P_2 (P-3516)
PtdIns(3)P (P-3016)	○	○	PtdIns(4,5)P_2 (P-4516)
PtdIns(4)P (P-4016)	○	○	PtdIns(3,4,5)P_3 (P-3916)
PtdIns(5)P (P-5016)	○	○	Phosphatidic Acid PA
Phosphatidylethanolamine PE	○	○	Phosphatidylserine PS
Phosphatidylcholine PC	○	○	Blank

B

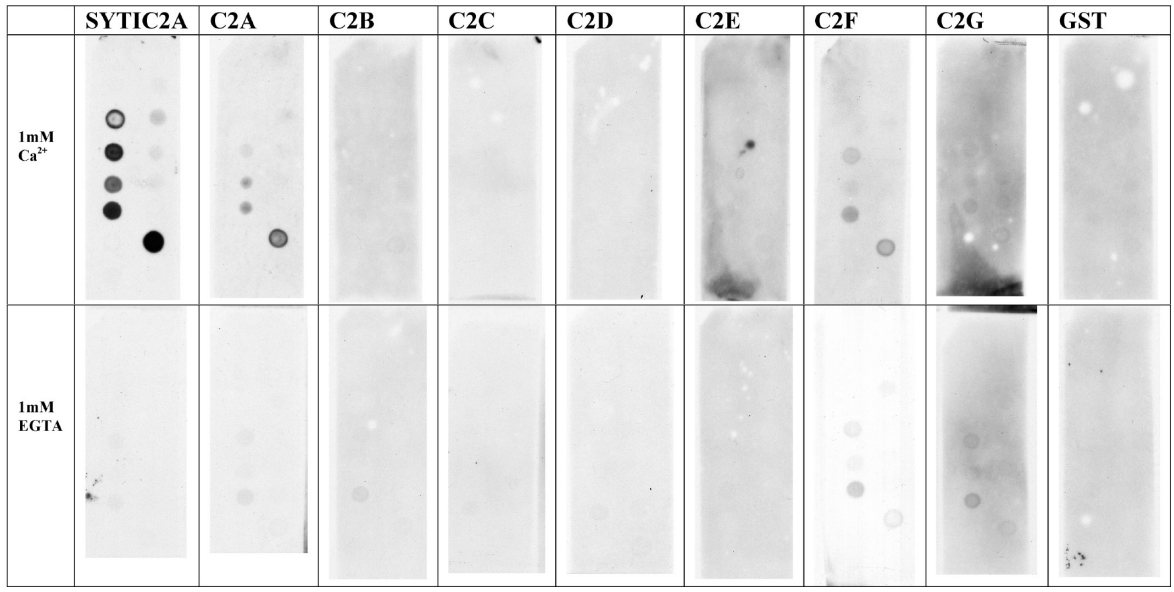

FIGURE 3: Lipid specificity and Ca^{2+} dependence of lipid binding of dysferlin C2 domains analyzed with protein−lipid overlay assays. (A) Listing of lipids found in the Echelon lipid strips. Each spot contains 100 pmol of lipid. (B) GST−C2 domain fusion proteins from dysferlin and synaptotagmin I were incubated with lipid strips in the presence of 1 mM Ca^{2+} or 1 mM EGTA. Interactions were revealed with anti-GST antibodies and chemiluminescence.

binding to PC or phosphatidylethanolamine, indicating that anionic lipids are preferred over neutral lipids. To increase the sensitivity of the assay, we prepared lipid strips with larger amounts of lipids. We used amounts that were up to 10-fold higher than those in the commercially available strips. We observed that all dysferlin C2 domains bound to PS (Figure 4B). However, only the C2A domains of synaptotagmin I and dysferlin exhibited Ca^{2+}-dependent PS binding, while the other dysferlin C2 domains demonstrated Ca^{2+}-independent PS binding (Figure 4B). To further characterize the PS interactions, we performed phospholipid centrifugation binding assays. In agreement with the data given above, the C2A domains of dysferlin and synaptotagmin I exhibited Ca^{2+}-dependent PS/PC vesicle binding (Figure 5). Approximately 50% of the synaptotagmin I C2A domain and 40% of the dysferlin C2A domain bound to PS/PC vesicles in the presence of 1 mM Ca^{2+}. In the absence of Ca^{2+}, the strength of this interaction was reduced 4-fold for the synaptotagmin I C2A domain and 2-fold for the dysferlin C2A domain. All of the other dysferlin C2 domains exhibited very weak lipid binding in a Ca^{2+}-independent manner (Figure 5). The control GST protein did not bind to PS/PC vesicles in the presence or absence of Ca^{2+} (<2% lipid-bound protein).

The C2A Domain of Dysferlin Binds Phosphoinositides in a Ca^{2+}-Dependent Fashion. In addition to PS binding, we observed Ca^{2+}-dependent binding of PtdIns(5)P and PtdIns(4)P with the dysferlin C2A domain (Figure 3B). The synaptotagmin I C2A domain also binds these lipids, as well as PtdIns(3)P and phosphoinositide, all in a Ca^{2+}-dependent manner (Figure 3B). Importantly, we did not observe any binding between PtdIns(4,5)P_2 and the synaptotagmin I C2A domain, which are known to interact in vitro (*18, 19*). Since the commercial lipid blots have very limited sensitivity, weak lipid binding domains could have gone undetected using them. Therefore, we repeated the experiment with our custom-made lipid strips blotted with several lipid concentrations to unequivocally show a lipid interaction. We were able to demonstrate detectable binding of the synaptotagmin I C2A domain to 625 pmol of PtdIns(4,5)P_2; this amount was 6-fold greater than the amount found on the commercial blot (100 pmol) (Figure 6). Ca^{2+}-dependent binding to PtdIns(4)P and PtdIns(4,5)P_2 was observed for the C2A domain of dysferlin (Figure 6), while no phosphoinositide interactions were detected with the other dysferlin C2 domains in the presence or absence of Ca^{2+} (data not shown). The Ca^{2+}-dependent binding of PtdIns(4)P and PtdIns(4,5)P_2 with the synaptotagmin C2A domain is consistent with previous reports (*17*−*19*).

We next performed Ca^{2+} titration experiments of phospholipid binding to determine the apparent Ca^{2+} affinities of phospholipid binding. The apparent Ca^{2+} affinity for PS binding was ~10 μM for both synaptotagmin and dysferlin C2A domains (Figure 7). This is in accordance with previously published data showing an apparent Ca^{2+} affinity value of 5 μM for the synaptotagmin I C2A domain and PS, while a half-maximal lipid binding value of 4.5 μM was reported for the dysferlin C2A domain (*13, 17*).

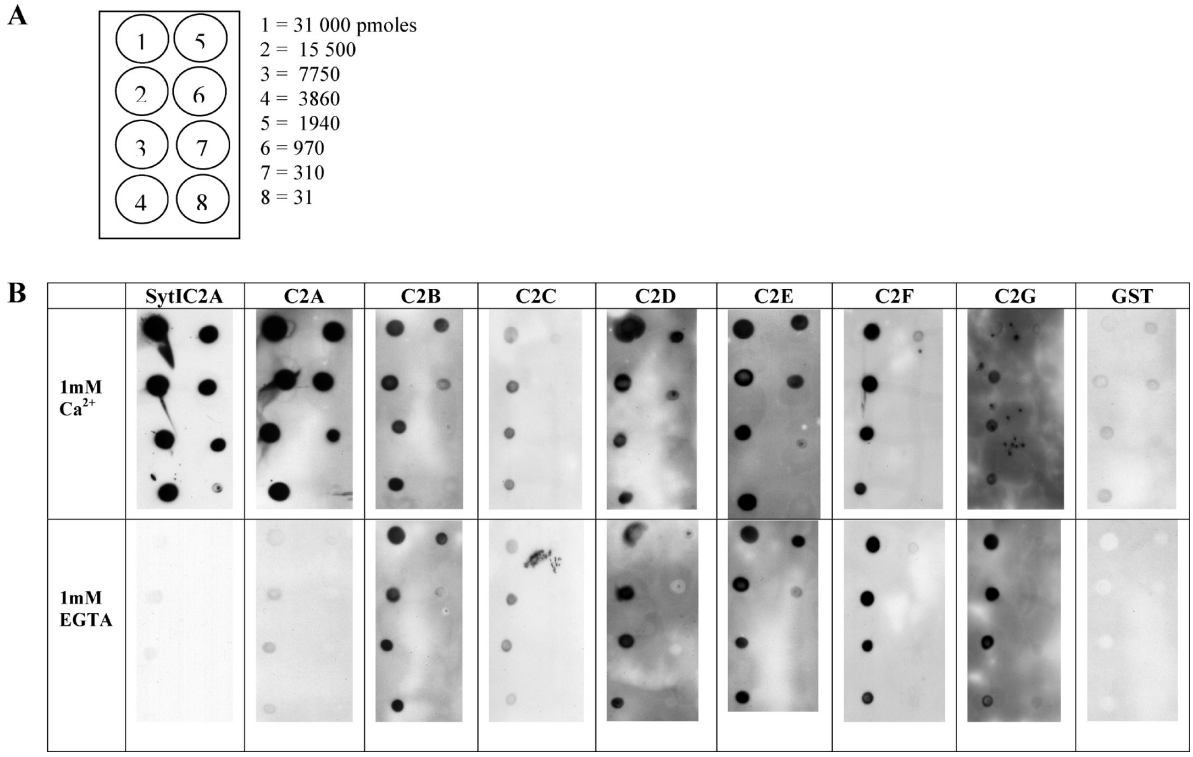

FIGURE 4: Ca^{2+}-dependent PS binding by dysferlin C2 domains determined with PLO assays. (A) Each spot contains between 31000 and 31 pmol of PS. (B) GST−C2 domain fusion proteins from dysferlin and synaptotagmin I were incubated with lipid strips in the presence of 1 mM Ca^{2+} or 1 mM EGTA. Interactions were revealed with anti-GST antibodies and chemiluminescence.

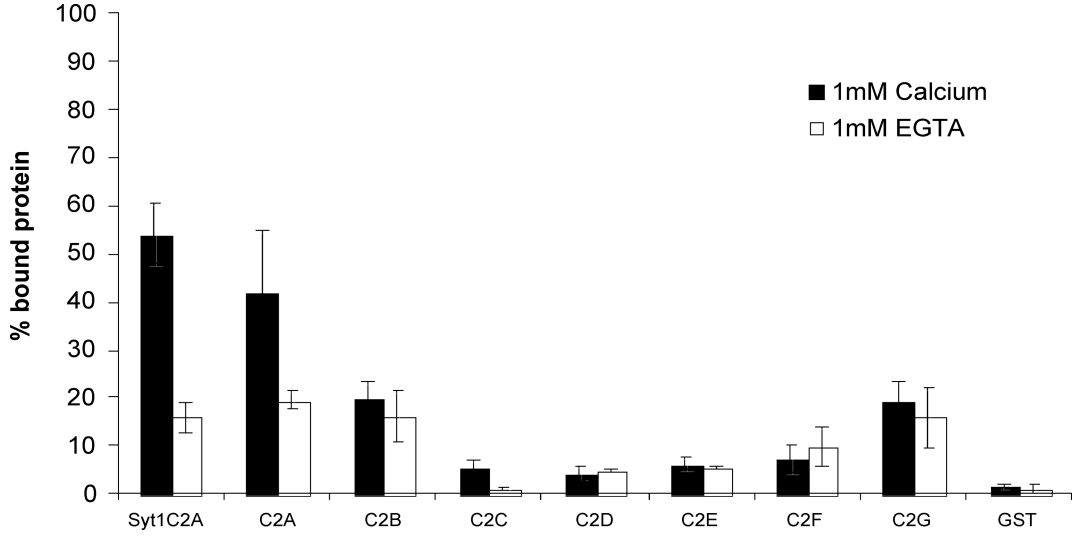

FIGURE 5: Ca^{2+}-dependent phospholipid binding to PS/PC vesicles by dysferlin C2 domains measured by a liposome centrifugation assay. GST−C2 domain fusion proteins were incubated with sucrose-loaded vesicles (65:35 PS/PC) in the presence of 1 mM Ca^{2+} or 1 mM EGTA. The samples were centrifuged and washed, and the bound protein was analyzed by SDS−PAGE and SimplyBlue SafeStain staining. The percentage of lipid-bound protein was determined as mentioned in Experimental Procedures. Mean values and the standard deviation were derived from triplicate experiments.

We found apparent Ca^{2+} affinity values for PtdIns(4)P and PtdIns(4,5)P_2 binding to the dysferlin C2A domain of 10 and 1 μM, respectively, whereas synaptotagmin I C2A domain's apparent Ca^{2+} affinities for PtdIns(4)P and PtdIns(4,5)P_2 binding were lower than that of dysferlin, with values of 50 and 10 μM, respectively (Figure 7).

DISCUSSION

Dysferlin's membrane binding function is thought to be mediated, in a manner analogous to that of synaptotagmins, by its multiple C2 domains. According to the patch model of membrane repair, Ca^{2+} influx near membrane disruption sites would activate dysferlin C2 domains, which in turn would trigger a series of fusion and/or recruitment events between cytoplasmic vesicles and the plasma membrane (*7*). The accumulation of these fused membranes underneath the sarcolemmal disruption site would create the membrane patch. The role of each individual dysferlin C2 domain in this process in not known. In this study, we evaluated the lipid binding specificities and the Ca^{2+} requirement of the seven C2 domains of dysferlin. Our data indicate that all of dysferlin's C2 domains are able to bind to PS. However,

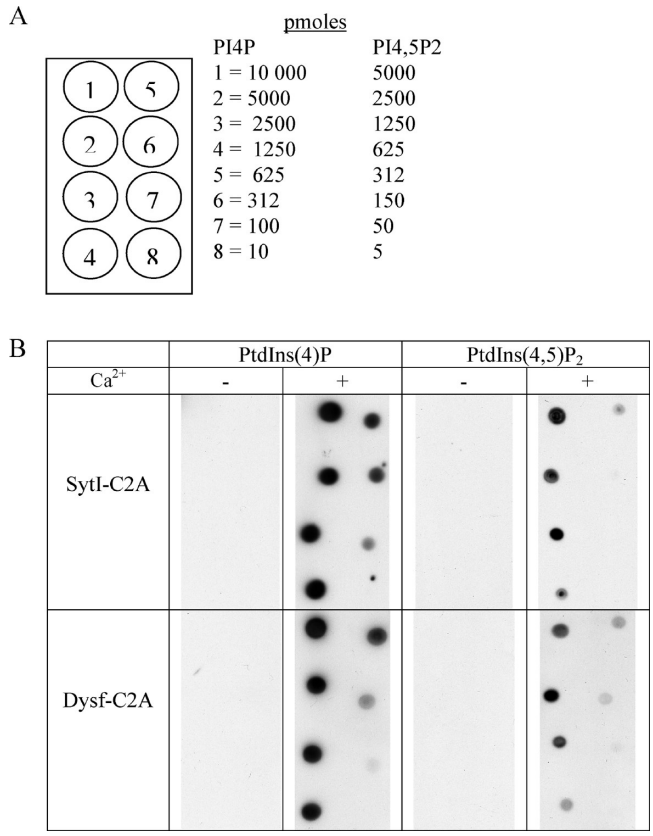

FIGURE 6: Ca^{2+}-dependent binding of PtdIns(4)P and PtdIns(4,5)P_2 by synaptotagmin I and dysferlin C2A domains analyzed with a protein−lipid overlay assay. (A) Each spot contains between 10000 and 5 pmol of phosphoinositides. (B) GST−C2A domain fusion proteins from dysferlin and synaptotagmin I were incubated with lipid strips in the presence of 1 mM Ca^{2+} or 1 mM EGTA. Interactions were revealed with anti-GST antibodies and chemiluminescence.

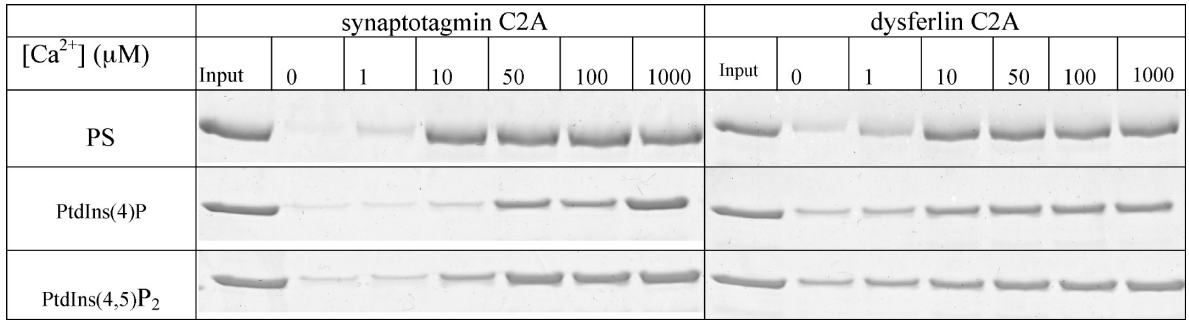

FIGURE 7: Ca^{2+} titration of phospholipid binding of the dysferlin C2A domain measured with liposome centrifugation assays. GST−C2A domain fusion proteins were incubated with sucrose-loaded vesicles (65:35 PS/PC, 20:80 PtdIns(4)P/PC, or 20:80 PtdIns(4,5)P_2/PC) in the presence of HEPES buffer and various Ca^{2+} concentrations obtained with clamped Ca^{2+}/EGTA buffers. The samples were centrifuged and washed, and the bound protein was analyzed by SDS−PAGE and SimplyBlue SafeStain staining.

only the C2A domain binds to PS and phosphoinositides in a Ca^{2+}-dependent fashion, and it binds more strongly than the other C2 domains, as judged by the liposome centrifugation experiment. Curiously, we did not observe a direct relationship between the number of Ca^{2+} binding residues and the calcium dependency of lipid binding in any of the seven C2 domains. The C2A domain of dysferlin contains three Asp residues and one Glu residue for a total of four negatively charged residues, one fewer than the five canonical Asp residues found in classical Ca^{2+}-dependent C2 domains. The C2B and C2E domains harbor two and one Asp residue, respectively, and are thus not predicted to bind several Ca^{2+} ions. However, all the other C2 domains contain four or more Asp/Glu residues but still display Ca^{2+}-independent PS binding. The C2B domain of rat synaptotagmin IV contains all five Asp residues, but as opposed to the fly othologue, it does not bind Ca^{2+} ions and is therefore considered not to be a Ca^{2+} switch in rodents (*20*). Analysis of the rat synaptotagmin IV C2B crystal structure revealed that changes in the orientations of critical Ca^{2+} ligands render the C2B domain unable to form full Ca^{2+} binding sites (*20*). It appears that the Ca^{2+} binding properties of C2 domains cannot be reliably predicted from sequence analyses alone but, rather, must be addressed by biochemical and functional studies. Future molecular studies, such as Ca^{2+} binding studies of individual dysferlin C2 domain fusion proteins, could shed light on whether some C2 domains are capable of binding Ca^{2+} without binding phospholipids.

Ca^{2+}-dependent binding of the two phosphoinositides, PtdIns(4)P and PtdIns(4,5)P_2, to the C2A domain of dysferlin was detected and characterized in this study for the first time. PtdIns(4)P is the most abundant phosphoinositide species in

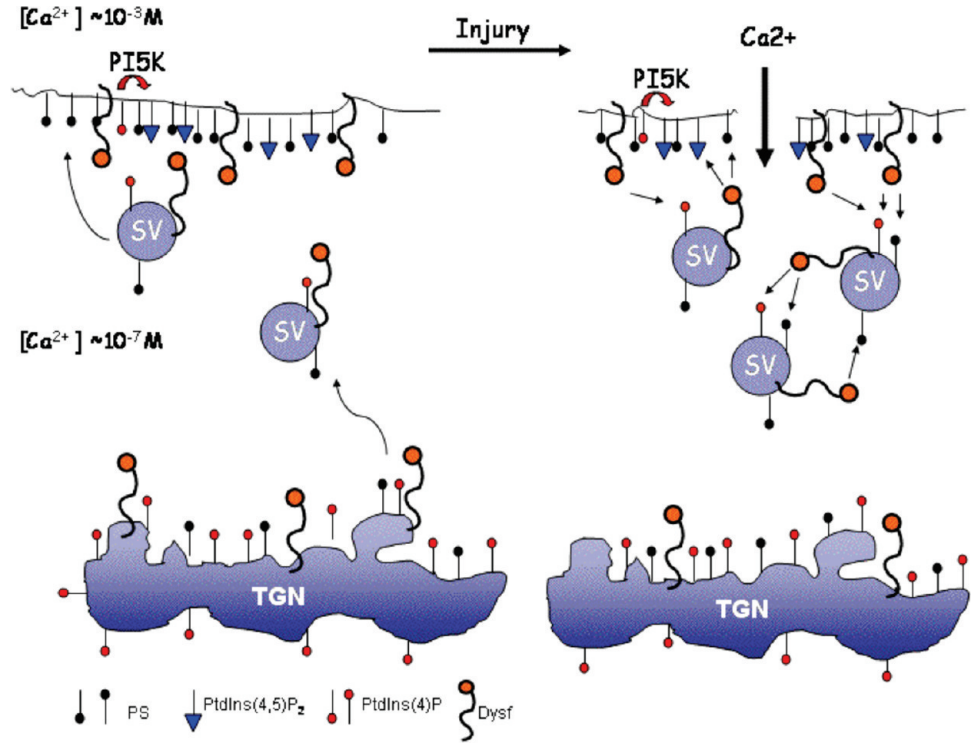

FIGURE 8: Schematic representation of proposed interactions of dysferlin with PS and phosphoinositides in injured cells. Upon membrane injuries, there is an inward flow of Ca^{2+} into the cells, which activates the C2A domain of dysferlin. Plasma membrane dysferlin interacts with vesicular PS and PtdIns(4)P, while vesicular dysferlin interacts with plasma membrane PS and PtdIns(4,5)P_2. In addition to these events, intervesicular interactions between dysferlin and PS or PtdIns(4)P generate membrane patches which are needed to reseal the membrane tears. TGN is the trans Golgi network. SV is secretory vesicle. PI5K is phosphatidylinositol 5-kinase.

mammalian cells and is found predominantly in the trans-Golgi network (TGN) (*21*). PtdIns(4)P is also found in the T-tubule system and terminal cisternae of the sarcoplasmic reticulum of skeletal muscle (*22*). PtdIns(4)P is implicated in the Golgi membrane docking of FAPP-1, FAPP-2, and CERT (*23*). Cargo protein FAPP (four-phosphatase-adaptor protein) is implicated in vesicle trafficking from the TGN to the plasma membrane in MDCK and COS cells (*24, 25*). PtdIns(4)P is phosphorylated in the plasma membrane by PI4P5K to yield PtdIns(4,5)P_2 (*21*). PtdIns(4,5)P_2 is found in the plasma membrane and in the T-tubule system of skeletal muscle (*22*). PtdIns(4,5)P_2 is an important precursor of signaling metabolites and is implicated in the regulation of actin regulatory proteins, cell adhesion molecules, clathrin adaptors, ion channels, and kinesins (*21*). PtdIns(4,5)P_2 was shown to coactivate Ca^{2+}-dependent and -independent phospholipid binding to synaptotagmin I C2 domains and to augment the Ca^{2+}- and PS-dependent membrane binding of the PKCα C2 domain by slowing its membrane dissociation (*18, 26*).

The molecular basis for dysferlin distribution and function in muscle cells might involve interactions with these phosphoinositides. As for synaptotagmin I, PtdIns(4,5)P_2 interactions might enable dysferlin to enhance its membrane binding activity in vivo. The SNARE protein syntaxin 1 was shown to directly bind and sequester fusogenic lipids like PtdIns(4,5)P_2 to the site of membrane fusion via a polybasic juxtamembrane region (*27*). Otoferlin, a member of the ferlin family, was shown to bind to SNAP-25 and syntaxin 1 in the presence of Ca^{2+} in the auditory ribbon synapse (*14*). By analogy, dysferlin could sequester fusogenic lipids alone or in combination with other sequestering proteins in the sarcolemma to enhance or initiate the fusion process mediated by the SNARE complex.

It appears that the C2A domain of dysferlin is the only Ca^{2+}-dependent lipid binding C2 domain that might be important for Ca^{2+}-dependent membrane interactions in muscle. The role of the other Ca^{2+}-independent phospholipid binding C2 domains of dysferlin is less clear at this time, but they may modulate the membrane binding activity of the C2A domain in a fashion similar to that of the tandem C2 domains of synaptotagmin I (*28, 29*).

In the case of a surface membrane injury, we propose that the Ca^{2+}-dependent interactions with PS and/or PtdIns(4,5)P_2 could trigger membrane interactions between the plasma membrane and subsarcolemmal dysferlin vesicles. The same interactions with PS and PtdIns(4)P could trigger intervesicular interactions and generate patches to quickly reseal the membrane tears (Figure 8). Although the in vitro conditions used in this study may not reflect physiological conditions found in quiescent muscle cells, they could be found in injured or stimulated cells through a local concentration effect (*30*). Hence, future in vivo studies will be required to substantiate these proposed mechanisms.

This study lays ground for future investigations into possible additional lipid or protein binding partners for dysferlin C2 domains and for functional in vivo studies.

ACKNOWLEDGMENT

We thank Dr. K. Bushby for the dysferlin cDNA. We thank Drs. C. Abi-Farah and W. Sossin for help with the liposome centrifugation assay and Dr. P. McPherson for helpful discussion.

REFERENCES

1. Bashir, R., Britton, S., Strachan, T., Keers, S., Vafiadaki, E., Lako, M., Richard, I., Marchand, S., Bourg, N., Argov, Z., Sadeh, M.,

Mahjneh, I., Marconi, G., Passos-Bueno, M. R., Moreira Ede, S., Zatz, M., Beckmann, J. S., and Bushby, K. (1998) A gene related to *Caenorhabditis elegans* spermatogenesis factor fer-1 is mutated in limb-girdle muscular dystrophy type 2B. *Nat. Genet. 20*, 37–42.
2. Liu, J., Aoki, M., Illa, I., Wu, C., Fardeau, M., Angelini, C., Serrano, C., Urtizberea, J. A., Hentati, F., Hamida, M. B., Bohlega, S., Culper, E. J., Amato, A. A., Bossie, K., Oeltjen, J., Bejaoui, K., McKenna-Yasek, D., Hosler, B. A., Schurr, E., Arahata, K., de Jong, P. J., and Brown, R. H., Jr. (1998) Dysferlin, a novel skeletal muscle gene, is mutated in Miyoshi myopathy and limb girdle muscular dystrophy. *Nat. Genet. 20*, 31–36.
3. Illa, I., Serrano-Munuera, C., Gallardo, E., Lasa, A., Rojas-García, R., Palmer, J., Gallano, P., Baiget, M., Matsuda, C., and Brown, R. H. (2001) Distal anterior compartment myopathy: A dysferlin mutation causing a new muscular dystrophy phenotype. *Ann. Neurol. 49*, 130–134.
4. Bansal, D., Miyake, K., Vogel, S. S., Groh, S., Chen, C. C., Williamson, R., McNeil, P. L., and Campbell, K. P. (2003) Defective membrane repair in dysferlin-deficient muscular dystrophy. *Nature 423*, 168–172.
5. Therrien, C., Dodig, D., Karpati, G., and Sinnreich, M. (2006) Mutation impact on dysferlin inferred from database analysis and computer-based structural predictions. *J. Neurol. Sci. 250*, 71–78.
6. Hernández-Deviez, D. J., Martin, S., Laval, S. H., Lo, H. P., Cooper, S. T., North, K. N., Bushby, K., and Parton, R. G. (2006) Aberrant dysferlin trafficking in cells lacking caveolin or expressing dystrophy mutants of caveolin-3. *Hum. Mol. Genet. 15*, 129–142.
7. Han, R., and Campbell, K. P. (2007) Dysferlin and muscle membrane repair. *Curr. Opin. Cell Biol. 19*, 409–416.
8. Min, S. W., Chang, W. P., and Südhof, T. C. (2007) E-Syts, a family of membranous Ca^{2+}-sensor proteins with multiple C2 domains. *Proc. Natl. Acad. Sci. U.S.A. 104*, 3823–3828.
9. Schulz, T. A., and Creutz, C. E. (2004) The tricalbin C2 domains: Lipid-binding properties of a novel, synaptotagmin-like yeast protein family. *Biochemistry 43*, 3987–3995.
10. Shin, O. H., Han, W., Wang, Y., and Südhof, T. C. (2005) Evolutionarily conserved multiple C2 domain proteins with two transmembrane regions (MCTPs) and unusual Ca^{2+} binding properties. *J. Biol. Chem. 280*, 1641–1651.
11. Tucker, W. C., and Chapman, E. R. (2002) Role of synaptotagmin in Ca^{2+}-triggered exocytosis. *Biochem. J. 366*, 1–13.
12. Cho, W., and Stahelin, R. V. (2006) Membrane binding and subcellular targeting of C2 domains. *Biochim. Biophys. Acta 1761*, 838–849.
13. Davis, D. B., Doherty, K. R., Delmonte, A. J., and McNally, E. M. (2002) Calcium-sensitive phospholipid binding properties of normal and mutant ferlin C2 domains. *J. Biol. Chem. 277*, 22883–22888.
14. Roux, I., Safieddine, S., Nouvian, R., Grati, M., Simmler, M. C., Bahloul, A., Perfettini, I., Le Gall, M., Rostaing, P., Hamard, G., Triller, A., Avan, P., Moser, T., and Petit, C. (2006) Otoferlin, defective in a human deafness form, is essential for exocytosis at the auditory ribbon synapse. *Cell 127*, 277–289.
15. Nalefski, E. A., and Falke, J. J. (1996) The C2 domain calcium-binding motif: Structural and functional diversity. *Protein Sci. 5*, 2375–2390.
16. Pepio, A. M., and Sossin, W. S. (2001) Membrane translocation of novel protein kinase Cs is regulated by phosphorylation of the C2 domain. *J. Biol. Chem. 276*, 3846–3855.
17. Shin, O. H., Rizo, J., and Südhof, T. C. (2002) Synaptotagmin function in dense core vesicle exocytosis studied in cracked PC12 cells. *Nat. Neurosci. 5*, 649–656.
18. Li, L., Shin, O. H., Rhee, J. S., Araç, D., Rah, J. C., Rizo, J., Südhof, T., and Rosenmund, C. (2006) Phosphatidylinositol phosphates as co-activators of Ca^{2+} binding to C2 domains of synaptotagmin 1. *J. Biol. Chem. 281*, 15845–15852.
19. Zhang, X., Rizo, J., and Südhof, T. C. (1998) Mechanism of phospholipid binding by the C2A-domain of synaptotagmin I. *Biochemistry 37*, 12395–12403.
20. Dai, H., Shin, O. H., Machius, M., Tomchick, D. R., Südhof, T. C., and Rizo, J. (2004) Structural basis for the evolutionary inactivation of Ca^{2+} binding to synaptotagmin 4. *Nat. Struct. Mol. Biol. 11*, 844–849.
21. Sasaki, T., Sasaki, J., Sakai, T., Takasuga, S., and Suzuki, A. (2007) The physiology of phosphoinositides. *Biol. Pharm. Bull. 30*, 1599–1604.
22. Milting, H., Heilmeyer, L. M., Jr., and Thieleczek, R. (1994) Phosphoinositides in membranes that build up the triads of rabbit skeletal muscle. *FEBS Lett. 345*, 211–218.
23. Yamaji, T., Kumagai, K., Tomishige, N., and Hanada, K. (2008) Two sphingolipid transfer proteins, CERT and FAPP2: Their roles in sphingolipid metabolism. *IUBMB Life 60*, 511–518.
24. Godi, A., Di Campli, A., Konstantakopoulos, A., Di Tullio, G., Alessi, D. R., Kular, G. S., Daniele, T., Marra, P., Lucocq, J. M., and De Matteis, M. A. (2004) FAPPs control Golgi-to-cell-surface membrane traffic by binding to ARF and PtdIns(4)P. *Nat. Cell Biol. 6*, 393–404.
25. Vieira, O. V., Verkade, P., Manninen, A., and Simons, K. (2005) FAPP2 is involved in the transport of apical cargo in polarized MDCK cells. *J. Cell Biol. 170*, 521–526.
26. Manna, D., Bhardwaj, N., Vora, M. S., Stahelin, R. V., Lu, H., and Cho, W. (2008) Differential roles of phosphatidylserine, PtdIns(4,5)P2, and PtdIns(3,4,5)P3 in plasma membrane targeting of C2 domains. Molecular dynamics simulation, membrane binding, and cell translocation studies of the PKCα C2 domain. *J. Biol. Chem. 283*, 26047–26058.
27. Lam, A. D., Tryoen-Toth, P., Tsai, B., Vitale, N., and Stuenkel, E. L. (2008) SNARE-catalyzed fusion events are regulated by Syntaxin1A-lipid interactions. *Mol. Biol. Cell 19*, 485–497.
28. Fuson, K. L., Montes, M., Robert, J. J., and Sutton, R. B. (2007) Structure of human synaptotagmin 1 C2AB in the absence of Ca^{2+} reveals a novel domain association. *Biochemistry 46*, 13041–13048.
29. Herrick, D. Z., Sterbling, S., Rasch, K. A., Hinderliter, A., and Cafiso, D. S. (2006) Position of synaptotagmin I at the membrane interface: Cooperative interactions of tandem C2 domains. *Biochemistry 45*, 9668–9674.
30. McLaughlin, S., Wang, J., Gambhir, A., and Murray, D. (2002) PIP(2) and proteins: Interactions, organization, and information flow. *Annu. Rev. Biophys. Biomol. Struct. 31*, 151–175.

BI802242R